A Platinum Open Access Journal for Organic Chemistry

Paper

Free to Authors and Readers | DOAJ Seal | *Arkivoc* **2023** (vii) 202312110

Rh^{III}-catalyzed synthesis and investigation of the DNA-binding properties of 11- and 13-substituted berberine derivatives

Philipp Groß, Phil M. Pithan, and Heiko Ihmels*

Department of Chemistry and Biology, and Center of Micro- and Nanochemistry and (Bio)Technology (Cμ), University of Siegen, Adolf-Reichwein-Str. 2, 57068 Siegen, Germany
Email: ihmels@chemie.uni-siegen.de

Received 10-14-2023 **Accepted Manuscript** 12-07-2023 **Published on line** 12-23-2023

Abstract

The Rh-catalyzed annulation reaction of 2-(ethynylaryl)ethaneamines was used as key step to synthesize two berberine derivatives with hydroxy and phenyl substituents in 11- and 13-position. These compounds showed absorption and emission properties comparable to the parent alkaloid berberine. The fluorescence of the hydroxy-substituted berberine (pK_a = 6.3) is efficiently quenched under acidic conditions, whereas a fluorescence light-up effect was observed with increasing pH values. The interactions of the berberine derivatives with duplex DNA and quadruplex DNA were investigated with absorption, circular dichroism (CD), and linear dichroism (LD) spectroscopy. The 13-phenyl-substituted berberine binds to duplex DNA with a binding constant of $K_b = 1.2 \times 10^5$ M^{-1} and to quadruplex DNA with $K_b = 1.9 \times 10^5$ M^{-1}. The CD- and LD-spectroscopic studies showed that the 11-hydroxy-13-phenyl-substituted berberine binds to duplex DNA by intercalation and to quadruplex DNA by terminal π-stacking.

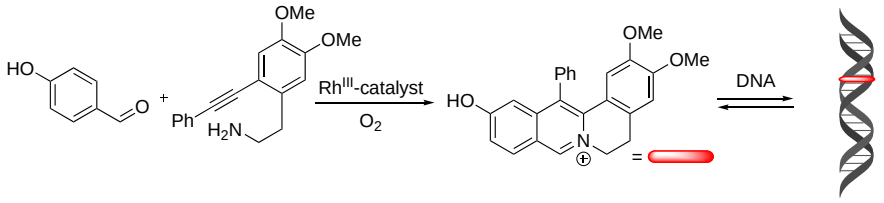

Keywords: *heterocycles*, *DNA recognition, hydroxyberberine, protoberberine*, *tetrahydroisoquinolinium*

Introduction

The tetrahydroisoquinoline scaffold is found in a broad range of alkaloids, which exhibit remarkable bioactivities.[1–3] Therefore, compounds with this structural feature are of great interest in medicinal chemistry and pharmaceutical sciences, and the exploration of novel pathways for the synthesis of tetrahydroisoquinoline derivatives allows the exploitation of novel analogues of these natural products.[1] Among the isoquinoline alkaloids, protoberberine derivatives, and especially berberine, are of particular interest, because they display a wide range of different biological activities, namely DNA-binding,[4–6] anticancer, antiviral and antiseptic properties.[7–9] Along these lines, the straightforward and variable synthesis of berberine derivatives provides important structures and lead compounds for the development of novel efficient and selective therapeutic agents.[8,10] Although several synthetic routes to berberine derivatives have been explored already,[8,9,11–13] many preparative approaches towards derivatization are limited to particular functional groups and often involve tedious multi-step synthesis.[12,14,15] Berberine itself is readily available in large quantities by extraction from plant material, but can only be readily functionalized in 9-, 9-*O*-, 10-*O*-, 12- and 13-position, so that a more versatile synthetic approach is necessary to provide a broader range of substitution patterns.[16–19] In this context, it has been shown that the annulation reaction of 2-(ethynylphenyl)ethaneamines and benzaldehydes through Rh-catalysis is a potent method for the synthesis of highly functionalized berberine derivatives from readily available precursors,[20,21] though terminal alkynes have not been applied, yet, and require silyl protection groups.[21] Hence, the Rh-catalyzed cyclization may facilitate the synthesis of berberine derivatives with novel substitution patterns and functional groups, which are inaccessible by conventional approaches.[21] In this context, the synthesis of hydroxy-substituted berberines figures as an attractive target, as hydroxy functionalities may have a significant effect on the bioactivity of a cationic hetarenes, which has already been shown in a comparison between berberine (**1a**) and the 9-hydroxy-substituted analogue berberrubine as well as for 12-hydroxy-substituted berberines.[22–24] In other studies, it has also been shown that the DNA-binding properties of resembling quinolizinium derivatives, such as the 8-hydroxybenzo[*b*]quinolizinium (**2a**) and 3-hydroxynaphtho[1,2-*b*]quinolizinium (**2b**), are influenced by the hydroxy functionality.[25,26] At the same time, the development of DNA-binding ligands is an important interdisciplinary research area because such compounds are promising candidates as lead structures for DNA-targeting drugs or as functional dyes for DNA detection.[27] Therefore, we focused our attention on novel hydroxyberberine derivatives to complement our ongoing studies of the factors that govern the DNA-binding properties of berberine derivatives.[18,28–30] And we proposed that the above-mentioned route through Rh-catalyzed annulation reaction may be employed as a key step for the synthesis, although hydroxy-substituted derivatives have not been prepared by this method, so far. Specifically, we investigated the synthesis of selected 11-hydroxyberberine derivatives **1b**, **1f**, and **1g**, and – for comparison – of a resembling reference compound without hydroxy group. Herein, we present the synthesis of 11-hydroxy-13-phenyl-substituted berberine and the corresponding "deoxy"-derivative along with their absorption, emission, and DNA-binding properties.

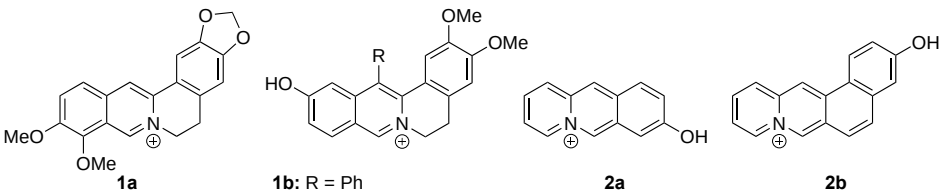

1a **1b:** R = Ph **1f:** R = TIPS (triisopropylsilyl) **1g:** R = H **2a** **2b**

Results and Discussion

Synthesis

Firstly, the amino group of homoveratrylamine (**3a**) was protected as acetamide **3b** by the reaction with trifluoroacetic ethylester (Scheme 1). Subsequent iodination with iodine chloride gave the iodo-substituted arene derivative **3c** in 81% yield over 2 steps.[14,31] The protected 2-iodohomoveratrylamine **3c** was employed in a Pd/Cu-mediated Sonogashira coupling reaction with alkynes **4a** or **4b** to yield the literature known alkynylated homoveratrylamine derivative **5a** and the novel derivative **5b** in 90% and 79% yield, respectively.[21] The amides **5a**,**b** were deprotected under alkaline conditions to give the free amines **6a** and **6b** in > 95% yield, respectively (Scheme 1). The structures of the known compounds **3a**–**c** and **6a**,**b** were confirmed with ^{1}H NMR spectroscopy and comparison with literature data.[14,21,31] Moreover, the structure of compound **5b** was unambiguously characterized by NMR spectroscopy (^{1}H, ^{13}C, H,H-COSY, HSQC and CH-HMBC), elemental analysis and mass spectrometry. Hence, the multiplicities and chemical shifts of proton signals at 1.15 ppm, 2.91 ppm and 2.98 ppm were assigned to the triisopropylsilyl group and the methylene groups. Furthermore, the singlets in the proton spectrum at 3.88 ppm, 3.89 ppm, 6.70 ppm and 6.95 ppm were assigned to the methoxy groups and the aromatic ring.

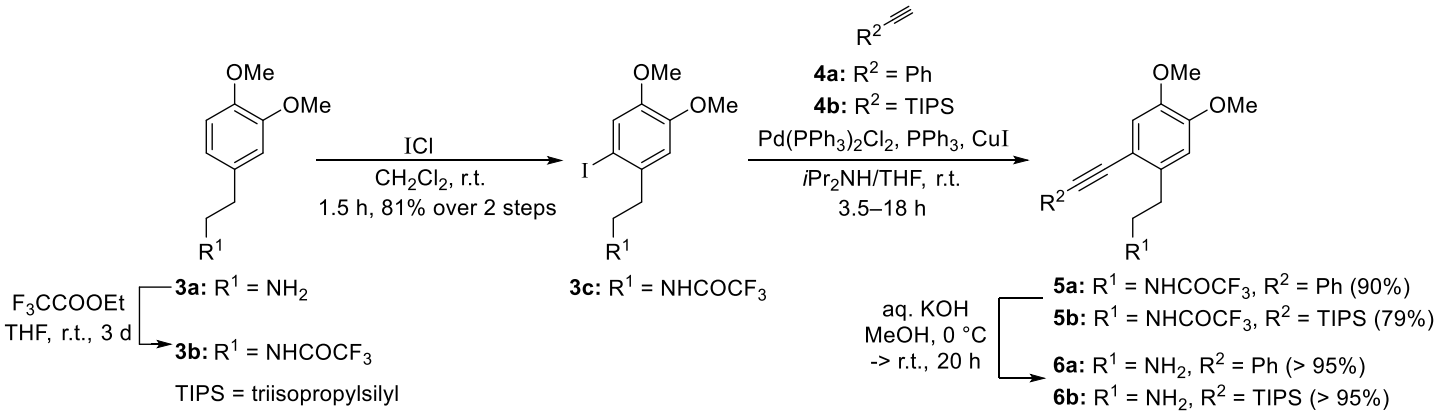

Scheme 1. Synthesis of the alkynylated homoveratrylamine derivatives **6a** and **6b**.

The phenylalkynyl-substituted homoveratrylamine **6a** was converted to the berberine derivates **1b** and **1c** in a Rh-catalyzed reaction with 4-hydroxybenzaldehyde (**7a**), benzaldehyde (**7b**), or 4-(triisopropylsilyloxy)-benzaldehyde (**7c**) in low yields of 16%, 8%, and 7%, respectively (Scheme 2).[21] In the case of the silyl-protected product obtained by the reaction with aldehyde **7c**, deprotection occurred during the chromatographic purification to directly give berberine **1b**.[32] However, the ^{1}H NMR-spectroscopic analysis of the crude product of **1b** indicated the initial formation of the TIPS-protected derivative. The novel berberine **1b** was fully characterized by NMR spectroscopy (^{1}H, ^{13}C, H,H-COSY, HSQC und CH-HMBC), elemental analysis, and mass spectrometry, showing characteristic proton signals at 3.03 ppm, 4.30 ppm, 5.62 ppm and 8.66 ppm, which were assigned to the methylene groups and the berberine framework. It should be noted, however, that the ^{1}H NMR shifts are concentration dependent. The structure of product **1c** was identified by comparison of the ^{1}H NMR-spectroscopic data with the literature data.[21] Thus, the characteristic triplets in the ^{1}H NMR spectrum at 3.25 ppm and 4.88 ppm were assigned to the methylene groups, while the signals at 7.46 ppm and 7.65 ppm were assigned to the phenyl ring. The elemental analysis showed that chloride was present as counter anion, which was presumably introduced during column-chromatographic purification on silica gel.

The Rh-catalyzed reaction of the silylalkynyl-substituted derivative **6b** and benzaldehyde (**7b**) led to the formation of berberine derivative **1e** (Scheme 2). The ^{1}H NMR-spectroscopic analysis indicated that the protected derivative **1d** was formed, but after chromatographic purification an additional ^{1}H NMR signal at 9.09 ppm appeared, which was assigned to the 13-H of the unsubstituted derivative **1e**. Hence, the berberine **1d** was presumably protodesilylated on the slightly acidic silica gel phase. In a second attempt, the crude product of berberine **1d** was directly deprotected by addition of trifluoroacetic acid (TFA) to give the product **1e** in 17% overall yield from the amine **6b** (Scheme 2).[33,34] In contrast, the reaction of 4-hydroxybenzaldehyde (**7a**) and silylalkynyl-substituted homoveratrylamine **6b** resulted in the formation of side products instead of the desired product **1f**, presumably because of the decomposition of the berberine during the purification process, as suggested by the ^{1}H NMR-spectroscopic analysis. The berberine **1e** was synthesized with a different counter ion when compared with the literature and was therefore unambiguously characterized by ^{1}H NMR spectroscopy, elemental analysis, and mass spectrometry.

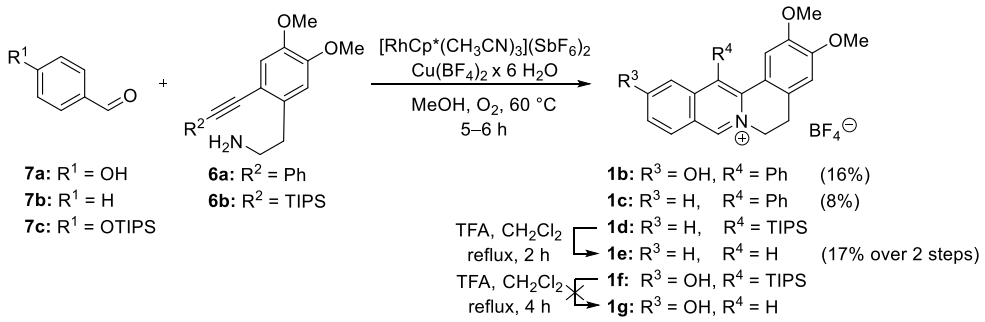

Scheme 2. Synthesis of berberines **1b**–**f** by a Rh-catalyzed annulation reaction.

Absorption and emission properties

The absorption and emission properties of the derivatives **1b** and **1e** were investigated in MeOH, DMSO, and $CHCl_3$ (Figure 1). The hydroxy-substituted berberine derivative **1b** showed a long-wavelength absorption band with a maximum at 379 nm in DMSO, 382 nm in $CHCl_3$, and 362 nm in MeOH, the latter, however, only as a very broad band. In addition, two slightly stronger, blue-shifted absorption maxima were observed at 318 nm and 293 nm in DMSO, at 312 nm and 294 nm in $CHCl_3$, and at 320 nm and 296 nm in MeOH (Figure 1, A1). Derivative **1c** showed emission maxima at 472 nm, 495 nm, and 490 nm in MeOH, DMSO, and $CHCl_3$, respectively. The fluorescence intensity was the highest in MeOH and the weakest in $CHCl_3$ (Figure 1, B1). The absorption spectrum of derivative **1e** in MeOH showed comparable features with a broad absorption at 380 nm and 340 nm (Figure 1, A2) and broad emission bands with low fluorescence intensity. The emission maximum is located at 435 nm in MeOH, at 461 nm in DMSO, and at 559 nm in $CHCl_3$ (Figure 1, B2). The absorption and emission properties closely resemble the ones of berberine (**1a**), however, the long- wavelength absorption maximum of berberine derivatives **1b** and **1e** is slightly blue-shifted and the absorption band is not as pronounced for **1e**, when compared to berberine (**1a**).[35]

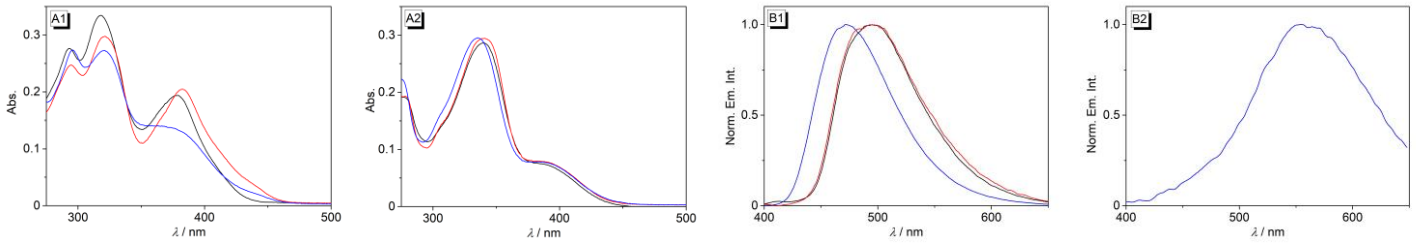

Figure 1. Absorption (A) and normalized emission spectra (B) of **1b** (1) (c = 20 µM, λ_{ex} = 350 nm) and **1e** (2) (c = 40 µM, λ_{ex} = 350 nm) in MeOH (blue), DMSO (black), $CHCl_3$ (red).

To assess the acidity of the hydroxy functionality of the berberine derivative **1b**, photometric and fluorimetric acid-base titrations were conducted in Britton-Robinson buffer (Figure 2). Thus, starting at pH 2, the solution was titrated with aq. NaOH solution (c = 2 M), and the acid-base reaction was monitored by absorption spectroscopy. During the titration, new absorption maxima at 313 and 373 nm were detected with increasing pH values (Figure 2A). Notably, no isosbestic points were formed, indicating that more than two absorbing species are formed in an acid-base equilibrium, namely the hydroxyberberine **1b**, its conjugate base and aggregates thereof. The derivative **1b** has a very weak emission in acidic medium with no distinct emission maximum. However, the emission intensity increased significantly, and a maximum at 468 nm developed with increasing pH value (Figure 2B). The plots of the absorption maximum at λ_{abs} = 373 nm and the fluorescence intensity at λ_{em} = 486 nm versus the pH value and a fit of the experimental titration curves to the Henderson-Hasselbalch equation revealed a pK_a value of 6.3 (Figure 2). Overall, the plots of the absorption and emission intensity of **1b** at a given wavelength versus the pH value of the solution showed the typical behavior of a cationic *N*-hetarene, namely a pronounced dependence of the absorption and emission properties on the pH because of the deprotonation of the hydroxy functionality in alkaline conditions, as also observed, for example, with hydroxybenzo[*b*]quinolizinium and 3-hydroxynaphthoquinolizinium.[25,26,36] A similar pH-dependent emission such as the one of **1b** has been reported for several hydroxynaphthalene derivatives and explained by the hydrogen bonds of the hydroxy functionality with the surrounding medium.[37,38] In contrast, however, the 9-hydroxy-substituted berberine derivative berberrubine shows a reverse trend, namely a broad emission band at λ_{max} = 550 nm in acidic medium, which is blue-shifted and quenched under alkaline conditions.[39] This different behavior of the two hydroxy-substituted berberine derivatives may be explained by fluorescence quenching in **1b** by a fast excited-state proton transfer reaction at the hydroxy functionality, which does not take place to significant extent in berberrubine.[40]

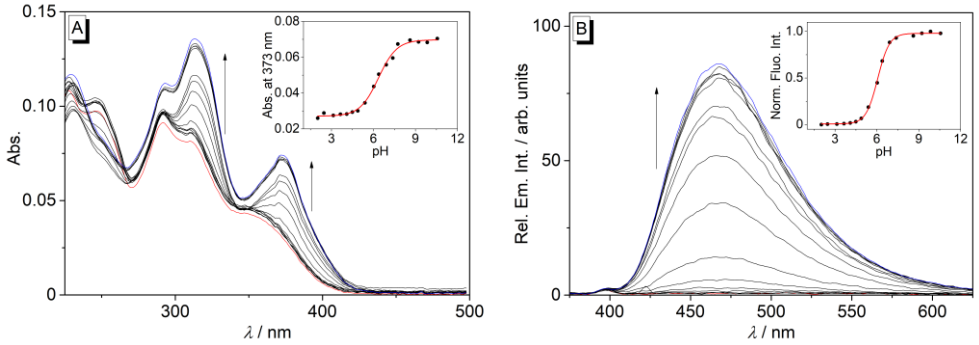

Figure 2. Photometric (A) and fluorimetric (B) acid-base titration of hydroxyberberine **1b** in Britton-Robinson buffer (c = 20 µM, pH = 2.0) with aq. NaOH solution (c = 2 M); λ_{ex} = 350 nm. The arrows indicate the change of the absorption or the emission during the titration. Red line: start of the titration; blue line: end of the titration. Inset: plot of the absorption at λ_{abs} = 373 nm (A) or the normalized fluorescence intensity at the emission maximum (corrected for change of the absorption at the excitation wavelength, λ_{ex} = 350 nm; λ_{em} = 468 nm) (B) versus the pH value; red lines: fitting of the experimental data to the theoretical curve of weak acids.

DNA binding properties

The binding interactions of berberine **1e** with calf thymus DNA (ct DNA) and quadruplex DNA d[A(GGGTTA)$_3$GGG] (**22AG**) were investigated with photometric DNA titrations. The addition of DNA to a solution of **1e** in phosphate buffer resulted in a decrease of the absorption and a red shift of the initial absorption maximum at 331 nm to 345 nm (ct DNA) and 341 nm (**22AG**), respectively (Figure 3, A and B). The titration data were used to determine the binding constants from the resulting binding isotherms and fitting of the experimental data to the theoretical non-competitive DNA binding model of Stootman et al. (Figure 4, A and B).[41] This analysis gave binding constants of $K_{ct\ DNA} = 1.2 \times 10^5\ M^{-1}$ for **1e** with ct DNA and $K_{\mathbf{22AG}} = 1.9 \times 10^5\ M^{-1}$ with quadruplex DNA **22AG**, which are in the commonly observed range of binding constants of berberine derivatives with these DNA forms.[42] For comparison, the parent compound berberine (**1a**) has binding constants of $K_{ct\ DNA} = 9.0 \times 10^3\ M^{-1}$ and $K_{\mathbf{22AG}} = 1.2 \times 10^6\ M^{-1}$.[43,44] Thus, the affinity of **1e** to quadruplex DNA **22AG** is lower than the one of berberine (**1a**), presumably because the lack of methoxy substituents changes the overall dipole of the ligand such that the attractive dipole-dipole interactions with the guanine quartet are reduced. In contrast, berberine (**1a**) binds weaker to duplex DNA than **1e** because the latter, smaller ligand fits much better into the intercalation site of ct DNA. Upon addition of DNA to a solution of hydroxyberberine **1b**, precipitation of the ligand-DNA complex occurred, so that the DNA-binding properties of this derivative could not be quantitatively assessed.

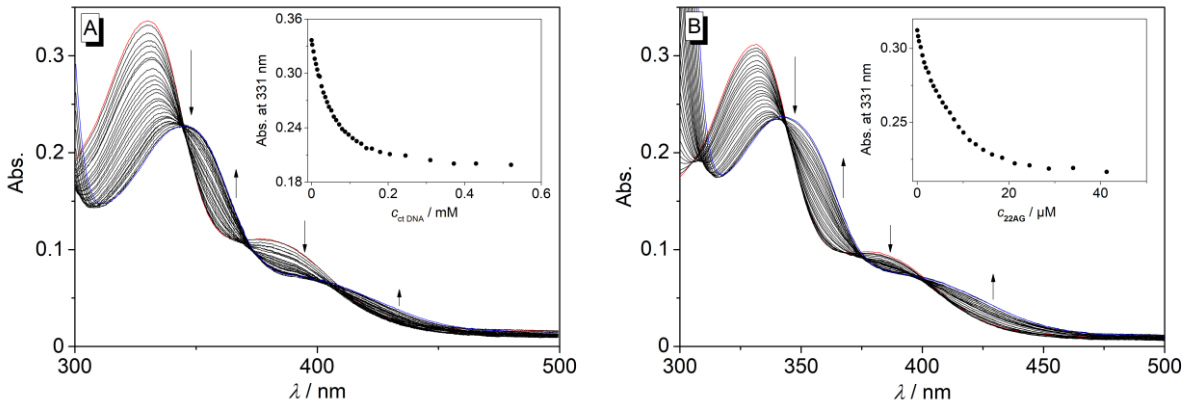

Figure 3. Photometric titration of **1e** with ct DNA (A) in BPE buffer ($c_{ct\ DNA}$ = 2.46 mM, c_{Na+} = 16 mM, pH = 7.0) and **22AG** (B) in KPB buffer [$c_{\mathbf{22AG}}$ = 190 µM, c_{K+} = 95 mM, pH = 7.0 with 5% DMSO (v/v)]. The arrows indicate the changes of absorption upon addition of DNA; red line: start of the titration, blue line: end of titration. Inset: plot of absorption at a defined wavelength versus the DNA concentration (c_{DNA} in base pairs/quartets).

Additionally, the interactions of **1b** with ct DNA and **22AG** were studied with circular dichroism (CD) spectroscopy (Figure 4A and 4B). The addition of ct DNA caused very broad negative induced CD (ICD) bands with peaks around 400 nm, 360 nm, and 320 nm, which were assigned to the long-wavelength absorption of the ligand **1e**. These ICD signals result from a non-degenerative coupling of transition dipoles of the ligand and the base pairs and thus confirm the complex formation.[45] Moreover, the negative band at 340 nm indicates a parallel alignment of the dipoles, which has also been observed for berberine (**1a**).[46] In the case of ct DNA, additional flow LD-spectroscopic studies were performed to further clarify the binding mode (Figure 4C).[45] Hence, a solution of ct DNA and ligand **1b** displayed an increasing negative LD band (> 300 nm) in the absorption region of the ligand with increasing ligand-to-DNA ratio. This negative LD band is unambiguous proof of intercalation because it indicates the coplanar alignment of the aromatic ligand relative to the base pairs, which also give a negative LD band at 254 nm.[45]

Upon addition of quadruplex DNA **22AG** to **1b**, a negative ICD signal developed at 318 nm. Additionally, a positive, but very weak ICD band developed at 383 nm, which suggests terminal π-stacking as binding mode of **1b** with a loose orientation of the ligand with respect to the transition moment of the adjacent base pairs.[45] The red-shifted ICD signal resembles that of known quadruplex-DNA-bound berberine derivatives,[29] while the negative ICD signal at 320 nm is usually not observed and may therefore be assigned to a specific transition that involves the phenyl substituent. Overall, these results are in agreement with terminal π-stacking to the quadruplex structure as predominant binding mode (Figure 4B).[45,47,48] This binding mode has been shown already for berberine (**1a**),[49] however, in that case, an association of two molecules in the binding site has been proposed, which is unlikely for **1b** because of the sterically demanding phenyl group in 13-position.

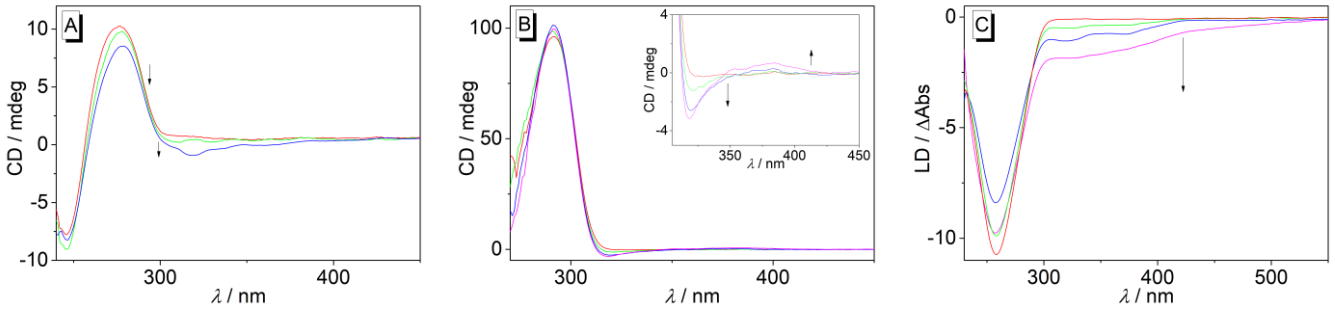

Figure 4. CD (A, B) and LD spectra (C) of solutions of **1b** and ct DNA (A, C) in BPE buffer solution [c_{Na+} = 16 mM, pH = 7.0 with 5% DMSO (v/v)] or **22AG** (B) in KPB buffer solution [$c_{\mathbf{22AG}}$ = 190 µM, c_{K+} = 95 mM, pH = 7.0 with 5% DMSO (v/v)]; LDR = 0 (red), 0.5 (green), 1.0 (blue), 1.5 (magenta). The arrows indicate the changes of the CD and LD bands upon addition of **1b.**

Conclusions

In summary, it was shown that the novel berberine derivatives **1b** and **1e** are available by the recently established Rh-catalyzed annulation reaction of the appropriate 2-(ethynylaryl)ethaneamines. But at the same time, it was observed that this method also has its limits, namely the hydroxy functionality in 11-position was only successfully introduced in combination with a phenyl substituent in 13-position, while the monosubstituted hydroxyberberine **1g** was not obtained. The novel berberines **1b** and **1e** essentially show the same absorption and emission properties as the parent compound berberine (**1a**). Furthermore, spectrometric acid-base titrations revealed a pK_a value of 6.3 for the hydroxyberberine **1b**, which is comparable with the pK_a of berberrubine (pK_a = 5–6), and an increase of the emission intensity with increasing pH value. Presumably, under acidic conditions the fluorescence of **1b** is efficiently quenched by a fast excited-state proton transfer reaction of the hydroxy group.[40,50] It was also shown that berberine **1e** exhibits a more pronounced binding affinity towards ct DNA than the parent compound berberine and binds to G4 DNA (ct DNA: $K_{\text{ct DNA}} = 1.2 \times 10^5$ M^{-1}; **22AG**: $K_{\mathbf{22AG}} = 1.9 \times 10^5$ M^{-1}). Additionally, intercalation or terminal π-stacking of **1e** as predominant binding mode towards both DNA forms was assessed by CD and LD spectroscopy, respectively. Therefore, this class of hydroxy-substituted protoberberines showed promising properties as potential DNA-binders with a pH-dependent emission, which is also known for other hydroxy-substituted cationic hetarenes.[25,26,36] Hence, the employed synthetic route provided functionalized tetrahydroisoquinolinium derivatives with promising photophysical and DNA-binding properties – although the yields are in need of improvement –, which are not readily available by "conventional" approaches.

Experimental Section

General. All reagents were commercially available and were used without further purification (*cf*. Supporting Information). The ^{1}H NMR spectra were recorded with a Bruker Avance 400 (^{1}H: 400 MHz, ^{13}C: 100 MHz) at room temperature (T = 25 °C). The ^{1}H NMR and ^{13}C NMR spectra were referenced to the residual proton signal of the solvent [DMSO-d_6: δ(^{1}H) = 2.50 ppm, δ(^{13}C) = 39.5 ppm or $CDCl_3$: δ(^{1}H) = 7.26 ppm, δ(^{13}C) = 77.2 ppm] and analyzed with the softwares ACD/NMR Processor and MestReNova. The elemental analyses were conducted in-

house at the University of Siegen, Organic Chemistry I. The mass spectra were measured with a Finnigan LCQ Deca (driving current: 6 kV, collision gas: argon, capillary temperature: 200 °C, support gas: nitrogen). The melting points were measured with a melting point apparatus BÜCHI 545 (Büchi, Flawil, CH) and are uncorrected. The sample solutions in the DNA experiments were mixed with a reaction vessel shaker Top-Mix 11118 (Fisher Bioblock Scientific). E-Pure® water was obtained with an ultrapure water system D4632-33 (Wilhelm Werner GmbH, Leverkusen, D) and the filters D 0835, D 0803 and D 5027 (2 ×). The pH values were measured with the pH measuring device QpH 70 (Merck). The absorption spectra were measured with Hellma quartz glass cuvettes 110-QS and 114B-QS (layer thickness d = 10 mm) on a Varian Cary 100 Bio-spectrophotometer, which was equipped with a thermostat. The emission spectra were measured with Hellma quartz glass cuvettes 115F-QS (layer thickness d = 10 mm) with a Varian Cary Eclipse fluorescence spectrometer, which was equipped with a thermostat. All measurements were recorded at T = 20 °C, if not stated otherwise. During the reactions, the solutions were stirred with a magnetic stirrer. Reaction temperatures refer to the medium surrounding the reaction vessel. The room temperature was 22 °C. The solvents were evaporated with a rotatory evaporator under reduced pressure.

***N*-(4,5-Dimethoxy-2-((triisopropylsilyl)ethynyl)phenethyl)-2,2,2-trifluoroacetamide (5b).**[14] Under inert gas atmosphere, iodotrifluoracetamide **3b** (2.02 g, 5.00 mmol) was added to a deaerated solution of triisopropylsilylacetylene (**4b**) (1.09 g, 6.00 mmol, 1.40 mL), $Pd(PPh_3)_2Cl_2$ (140 mg, 200 µmol), CuI (76.0 mg, 400 µmol) and PPh_3 (105 mg, 400 µmol) in anhydrous iPr$_2$NH/THF (1/1 v/v, 40 mL), and the reaction mixture was stirred at r.t. for 3.5 h. The reaction mixture was added to sat. aq. NH_4Cl solution (100 mL) and subsequently extracted with CH_2Cl_2 (3 × 80 mL). The combined organic layers were dried with Na_2SO_4, the drying agent was filtered off, and the solvent was removed under reduced pressure. The crude product was recrystallized from EtOAc/*n*-hexane to obtain amide **5b** as light-yellow solid (1.80 g, 3.93 mmol, 79%). For analytic purposes, the product was recrystallized from *n*-hexane; mp 70–75 °C. – ^{1}H NMR (400 MHz, $CDCl_3$): δ = 1.14 (s, 3 H, Si(C**H**$(CH_3)_2)_3$), 1.14 (s, 18 H, Si(CH(C**H**$_3)_2)_3$), 3.06 (t, ^3J = 7 Hz, 2 H, CH_2), 3.67 (t, ^3J = 6 Hz, 2 H, CH_2'), 3.87 (s, 3 H, 5-OCH_3), 3.89 (s, 3 H, 4-OCH_3), 6.35 (br. s, 1 H, NH), 6.64 (s, 1 H, 6-H), 6.96 (s, 1 H, 3-H). – ^{13}C NMR (100 MHz, $CDCl_3$): δ = 11.3 (Si(**C**H$(CH_3)_2)_3$), 18.7 (Si(CH(**C**H$_3)_2)_3$), 33.2 (CH_2), 40.4 (CH_2'), 55.9 (4-OCH_3), 56.1 (5-OCH_3), 93.6 (2-C**C**Si), 105.0 (2-**C**CSi), 112.1 (C6), 115.0 (C2), 115.2 (C3), 133.2 (C1), 147.6 (C4), 149.7 (C5). – MS (ESI$^+$): m/z (rel. intensity) = 937 (100) $[2\ M + Na]^+$, 480 (84) $[M + Na]^+$.

General procedure for the synthesis of 11- and 13-substituted berberine derivatives (GP 1).[21] In a sealed tube, a mixture of $Cu(BF_4)_2 \times 6\ H_2O$ (600 µmol) and $[RhCp^*(CH_3CN)_3](SbF_6)_2$ (25.0 µmol) was evacuated and flushed with O_2 (purity 4.8) three consecutive times. A solution of the arylaldehyde (1.20 mmol) and the homoveratrylamine **6a** or **6b** (1.00 mmol) in MeOH (8.5 mL) was added, and the reaction mixture was stirred at 60 °C for 5–6 h. The suspension was treated with CH_2Cl_2 (35 mL), filtered through a celite pad, and washed with CH_2Cl_2 (100 mL). The solvent was removed under reduced pressure, and the crude product was purified by column chromatography.

11-Hydroxy-2,3-dimethoxy-13-phenyl-5,6-dihydroisoquinolino[3,2-*a*]isoquinolin-7-ium (1b).[21] According to GP 1, a mixture of 2-(phenylethynyl)homoveratrylamine (**6a**) (294 mg, 1.04 mmol), 4-hydroxybenzaldehyde (**7a**) (147 mg, 1.20 mmol, 120 µL), $Cu(BF_4)_2 \times 6\ H_2O$ (207 mg, 600 µmol), $[RhCp^*(CH_3CN)_3](SbF_6)_2$ (20.8 mg, 25.0 µmol) in MeOH (8.5 mL) was stirred for 6 h. The crude product was purified by flash-column chromatography (SiO_2; CH_2Cl_2/MeOH, 95/5 v/v, R_f = 0.37), recrystallized from MeOH and washed with Et_2O to give the product **1b**-**Cl** as yellow amorphous solid (55.0 mg, 143 µmol, 14%); mp 293–297 °C (dec.). – ^{1}H NMR (400 MHz, DMSO-d_6): δ = 3.02–3.04 (m, 5 H, 3-OCH_3, 5-H), 3.74 (s, 3 H, 2-OCH_3), 4.28 (t, ^3J = 6 Hz, 2 H, 6-H), 5.60 (d, ^4J = 2 Hz, 1 H, 12-H), 6.38 (s, 1 H, 4-H), 6.59 (dd, ^3J = 9 Hz, ^4J = 2 Hz, 1 H, 10-H), 6.91 (s, 1 H, 1-H), 7.22–7.24

(m, 2 H,2'-H, 6'-H), 7.49–7.53 (m, 3 H, 3'-H, 4'-H, 5'-H), 7.58 (d, ^3J = 9 Hz, 1 H, 9-H), 8.64 (s, 1 H, 8-H). – ^{13}C NMR (100 MHz, DMSO-d_6): δ = 27.9 (C5), 53.1 (C6), 54.7 (2-OCH_3), 55.5 (3-OCH_3), 109.9 (C12), 110.7 (C4), 113.6 (C1), 114.9 (C8a), 120.0 (C13b), 124.5 (C13), 127.8 (C4'), 129.4 (C3', C5'), 130.6 (C2', C6'), 131.0 (C10), 131.2 (C4a), 131.2 (C9), 133.7 (C13a), 137.5 (C1'), 141.2 (C12a), 141.9 (C8), 146.0 (C2), 149.1 (C3), 179.9 (C11). – MS (ESI$^+$): *m*/*z* (rel. intensity) = 384 (100) [M − BF_4^-]$^+$, 406 (88) [M + Na^+ − H^+ − BF_4^-]$^+$. – El. Anal. for $C_{25}H_{22}NO_3Cl$ (419.90), calcd.: C 71.51, H 5.28, N 3.34; found: C 71.67, H 5.18, N 3.24.

2,3-Dimethoxy-5,6-dihydroisoquinolino[3,2-*a*]isoquinolin-7-ium (1e).[12,21] According to GP 1, a mixture 2-(triisopropylsilylethinyl)homoveratrylamine (**6b**) (84.4 mg, 233 µmol), benzaldehyde (**7b**) (38.2 mg, 360 µmol, 37.0 µL), $Cu(BF_4)_2 \times 6\ H_2O$ (62.1 mg, 180 µmol) and $[RhCp^*(CH_3CN)_3](SbF_6)_2$, (6.25 mg, 7.50 µmol) in MeOH (2.5 mL) was stirred for 5 h. The crude product was purified by flash-column chromatography (SiO_2; CH_2Cl_2/MeOH, 95/5 v/v, R_f = 0.30). The obtained solid (35.0 mg, 76.9 µmol) was redissolved in CH_2Cl_2 (1.0 mL) and TFA (351 mg, 3.08 mmol, 0.24 mL) and the mixture was stirred under reflux for 2 h. The reaction mixture was added dropwise to Et_2O (100 mL), the resulting precipitate was filtered off and washed with Et_2O to give the product **1e** as yellow amorphous solid (15.0 mg, 39.6 µmol, 17%), mp 245–246 °C (dec.). – ^{1}H NMR (400 MHz, DMSO-d_6): δ = 3.26 (t, ^3J = 6 Hz, 2 H, 5-H), 3.89 (s, 3 H, 3-OCH_3), 3.95 (s, 3 H, 2-OCH_3), 4.88 (t, ^3J = 6 Hz, 2 H, 6-H), 7.13 (s, 1 H, 4-H), 7.77 (s, 1 H, 1-H), 7.95−7.98 (m, 1 H, 10-H), 8.18–8.27 (m, 2 H, 11-H, 12-H), 8.42 (d, ^3J = 8 Hz, 1 H, 9-H), 9.09 (s, 1 H, 13-H), 10.00 (s, 1 H, 8-H). – MS (ESI$^+$): *m*/*z* (rel. intensity) = 292 (100) [M − BF_4^-]$^+$. – El. Anal. for $C_{19}H_{18}BF_4NO_2 \times H_2O$ (397.18), calcd.: C 57.46, H 5.08, N 3.53; found: C 57.77, H 4.88, N 3.58.

Acknowledgements

Generous support by the Deutsche Forschungsgesellschaft (Ih24/17-1) and the University of Siegen is gratefully acknowledged. We thank Rochus Breuer for the CHNS analysis. We thank Sandra Uebach for the CD- and LD-spectroscopic measurements.

Supplementary Material

Supplementary material (SI) is available.

References

1. Kim A. N.; Ngamnithiporn A.; Du E.; Stoltz B. M. *Chem. Rev.* **2023**, *123*, 9447–9496. https://doi.org/10.1021/acs.chemrev.3c00054
2. Ge H.; Zhang W.; Yuan K.; Xue H.; Cheng H.; Chen W.; Xie Y.; Zhang J.; Xu X.; Yang P. *Eur. J. Med. Chem.* **2021**, *221*, 113522–113536. https://doi.org/10.1016/j.ejmech.2021.113522
3. Da-Cunha E. V. L.; Fechinei I. M.; Guedes D. N.; Barbosa-Filho J. M.; Da Silva M. S. *The Alkaloids* **2005**, *62*, 1–75.
4. Ma Y.; Ou T.-M.; Tan J.-H.; Hou J.-Q.; Huang S.-L.; Gu L.-Q.; Huang Z.-S. *Bioorg. Med. Chem. Lett.* **2009**, *19*, 3414–3417. https://doi.org/10.1016/j.bmcl.2009.05.030

5. Ma Y.; Ou T.-M.; Hou J.-Q.; Lu Y.-J.; Tan J.-H.; Gu L.-Q.; Huang Z.-S. *Bioorg. Med. Chem.* **2008**, *16*, 7582–7591. https://doi.org/10.1016/j.bmc.2008.07.029
6. Park K. D.; Lee J. H.; Kim S. H.; Kang T. H.; Moon J. S.; Kim S. U. *Bioorg. Med. Chem. Lett.* **2006**, *16*, 3913–3916. https://doi.org/10.1016/j.bmcl.2006.05.033
7. Tarabasz D.; Kukula-Koch W. *Phytother. Res.* **2020**, *34*, 33–50. https://doi.org/10.1002/ptr.6504
8. Sun H.; Huang S.-Y.; Jeyakkumar P.; Cai G.-X.; Fang B.; Zhou C.-H. *J. Med. Chem.* **2022**, *65*, 436–459. https://doi.org/10.1021/acs.jmedchem.1c01592
9. Sun Y.; Xun K.; Wang Y.; Chen X. *Anticancer Drugs* **2009**, *20*, 757–769. https://doi.org/10.1097/CAD.0b013e328330d95b
10. Gaba S.; Saini A.; Singh G.; Monga V. *Bioorg. Med. Chem.* **2021**, *38*, 116143–116162. https://doi.org/10.1016/j.bmc.2021.116143
11. Fu L.; Mou J.; Deng Y.; Ren X. *Front. Pharm.* **2022**, *13*, 940282–940296. https://doi.org/10.3389/fphar.2022.940282
12. Lahm G.; Deichmann J.-G.; Rauen A. L.; Opatz T. *J. Org. Chem.* **2015**, *80*, 2010–2016. https://doi.org/10.1021/jo502842s
13. Bhowmik D.; Buzzetti F.; Fiorillo G.; Orzi F.; Syeda T. M.; Lombardi P.; Suresh Kumar G. *Med. Chem. Commun.* **2014**, *5*, 226–231. https://doi.org/10.1039/c3md00254c
14. Mujahidin D.; Doye S. *Eur. J. Org. Chem.* **2005**, 2689–2693. https://doi.org/10.1002/ejoc.200500095
15. Bian X.; He L.; Yang G. *Bioorg. Med. Chem.* **2006**, *16*, 1380–1383. https://doi.org/10.1016/j.bmcl.2005.11.045
16. Bazzicalupi C.; Bonardi A.; Biver T.; Ferraroni M.; Papi F.; Savastano M.; Lombardi P.; Gratteri P. *Int. J. Mol. Sci.* **2022**, *23*, 14061–14076. https://doi.org/10.3390/ijms232214061
17. Chen J.; Duan Y.; Yu X.; Zhong J.; Bai J.; Li N.-G.; Zhu Z.; Xu J. *J. Enzym. Inhib. Med. Chem.* **2022**, *37*, 2423–2433. https://doi.org/10.1080/14756366.2022.2118268
18. Wickhorst P. J.; Blachnik M.; Lagumdzija D.; Ihmels H. *Beilstein J. Org. Chem.* **2021**, *17*, 991–1000. https://doi.org/10.3762/bjoc.17.81
19. Guamán Ortiz L. M.; Tillhon M.; Parks M.; Dutto I.; Prosperi E.; Savio M.; Arcamone A. G.; Buzzetti F.; Lombardi P.; Scovassi A. I. *BioMed Res. Int.* **2014**, 924585–924596. https://doi.org/10.1155/2014/924585
20. Upadhyay N. S.; Jayakumar J.; Cheng C.-H. *Chem. Commun.* **2017**, *53*, 2491–2494. https://doi.org/10.1039/C7CC00008A
21. Jayakumar J.; Cheng C.-H. *Chem. Eur. J.* **2016**, *22*, 1800–1804. https://doi.org/10.1002/chem.201504378
22. Kim S. A.; Kwon Y.; Kim J. H.; Muller M. T.; Chung I. K. *Biochem.* **1998**, *37*, 16316–16324. https://doi.org/10.1021/bi9810961
23. Jeon Y. W.; Jung J. W.; Kang M.; Chung K.; Lee W. *Bull. Korean Chem. Soc.* **2002**, *23*, 391–394. https://doi.org/10.5012/bkcs.2002.23.3.391

24. Villegas J.; Ball B. C.; Shouse K. M.; VanArragon C. W.; Wasserman A. N.; Bhakta H. E.; Oliver A. G.; Orozco-Nunnelly D. A.; Pruet J. M. *Beilstein J. Org. Chem.* **2023**, *19*, 1511–1524. https://doi.org/10.3762/bjoc.19.108
25. Schäfer K.; Ihmels H.; Bohne C.; Valente K. P.; Granzhan A. *J. Org. Chem.* **2016**, *81*, 10942–10954. https://doi.org/10.1021/acs.joc.6b01991
26. Becher J.; Berdnikova D. V.; Dzubiel D.; Ihmels H.; Pithan P. M. *Beilstein J. Org. Chem.* **2017**, *13*, 203–212. https://doi.org/10.3762/bjoc.13.23
27. Bhaduri S.; Ranjan N.; Arya D. P. *Beilstein J. Org. Chem.* **2018**, *14*, 1051–1086. https://doi.org/10.3762/bjoc.14.93
28. Wickhorst P. J.; Ihmels H. *Molecules* **2021**, *26*, 2566–2579. https://doi.org/10.3390/molecules26092566
29. Wickhorst P. J.; Ihmels H. *Chem. Eur. J.* **2021**, *27*, 8580–8589. https://doi.org/10.1002/chem.202100297
30. Becher J.; Berdnikova D. V.; Ihmels H.; Stremmel C. *Beilstein J. Org. Chem.* **2020**, *16*, 2795–2806. https://doi.org/10.3762/bjoc.16.230
31. Shi C.; Ojima I. *Tetrahedron* **2007**, *63*, 8563–8570. https://doi.org/10.1016/j.tet.2007.04.097
32. Otto N.; Ferenc D.; Opatz T. *J. Org. Chem.* **2017**, *82*, 1205–1217. https://doi.org/10.1021/acs.joc.6b02647
33. Boers R. B.; Randulfe Y. P.; van der Haas, H. N. S.; van Rossum-Baan M.; Lugtenburg J. *Eur. J. Org. Chem.* **2002**, *13*, 2094–2108. https://doi.org/10.1002/1099-0690(200207)2002:13<2094::AID-EJOC2094>3.0.CO;2-E
34. Davies S. G.; Goodfellow C. L. *J. Chem. Soc. Perkin Trans. 1* **1990**, *36*, 393–407. https://doi.org/10.1039/P19900000393
35. Megyesi M.; Biczók L. *J. Phys. Chem. B* **2007**, *111*, 5635–5639. https://doi.org/10.1021/jp067702g
36. Ihmels H.; Schäfer K. *Photochem. Photobiol. Sci.* **2009**, *8*, 309–311. https://doi.org/10.1039/b816048a
37. Henson R. M. C.; Wyatt P. A. H. *J. Chem. Soc., Faraday Trans. 2* **1975**, *71*, 669–681. https://doi.org/10.1039/f29757100669
38. Alazaly A. M.; Amer A. S.; Fathi A. M.; Abdel-Shafi A. A. *J. Photochem. Photobiol., A* **2018**, *364*, 819–825. https://doi.org/10.1016/j.jphotochem.2018.07.019
39. Delgado-Camón A.; Jarne C.; Cebolla V. L.; Larrañaga O.; Cózar A. de; Cossío F. P.; Vara Y.; Domínguez A.; Membrado L.; Galbán J.; Garriga R. *Tetrahedron* **2015**, *71*, 6148–6154. https://doi.org/10.1016/j.tet.2015.06.098
40. Kim J.-M.; Chang T.-E.; Kang J.-H.; Park K. H.; Han D.-K.; Ahn K.-D. *Angew. Chem. Int. Ed.* **2000**, *39*, 1780–1782. https://doi.org/10.1002/(SICI)1521-3773(20000515)39:10<1780::AID-ANIE1780>3.0.CO;2-H
41. Stootman F. H.; Fisher D. M.; Rodger A.; Aldrich-Wright J. R. *Analyst* **2006**, *131*, 1145–1151. https://doi.org/10.1039/b604686j
42. Bhowmik D.; Fiorillo G.; Lombardi P.; Kumar G. S. *J. Mol. Recognit.* **2015**, *28*, 722–730. https://doi.org/10.1002/jmr.2486
43. Bhadra K.; Kumar G. S. *Med. Res. Rev.* **2011**, *31*, 821–862. https://doi.org/10.1002/med.20202

44. Bhadra K.; Kumar G. S. *Biochim. Biophys. Acta, Gen. Subj.* **2011**, *1810*, 485–496. https://doi.org/10.1016/j.bbagen.2011.01.011
45. Šmidlehner T.; Piantanida I.; Pescitelli G. *Beilstein J. Org. Chem.* **2018**, *14*, 84–105. https://doi.org/10.3762/bjoc.14.5
46. Debnath D.; Kumar G. S.; Maiti M. *J. Biomol. Struct. Dyn.* **1991**, *9*, 61–79. https://doi.org/10.1080/07391102.1991.10507893
47. Yamashita T.; Uno T.; Ishikawa Y. *Bioorg. Med. Chem.* **2005**, *13*, 2423–2430. https://doi.org/10.1016/j.bmc.2005.01.041
48. Sun H.; Tang Y.; Xiang J.; Xu G.; Zhang Y.; Zhang H.; Xu L. *Bioorg. Med. Chem. Lett.* **2006**, *16*, 3586–3589. https://doi.org/10.1016/j.bmcl.2006.03.087
49. Jain A. K.; Bhattacharya S. *Bioconjugate Chem.* **2011**, *22*, 2355–2368. https://doi.org/10.1021/bc200268a
50. Spinozzi S.; Colliva C.; Camborata C.; Roberti M.; Ianni C.; Neri F.; Calvarese C.; Lisotti A.; Mazzella G.; Roda A. *J. Nat. Prod.* **2014**, *77*, 766–772. https://doi.org/10.1021/np400607k